International Journal of Mass Spectrometry 309 (2012) 192–199

Contents lists available at SciVerse ScienceDirect

International Journal of Mass Spectrometry

journal homepage: www.elsevier.com/locate/ijms

Electron ionization cross-section and fragmentation of α-cyclohexanedione

Anamika Mukhopadhyay, Arup Kumar Ghosh, Moitrayee Mukherjee, Tapas Chakraborty*

Department of Physical Chemistry, Indian Association for the Cultivation of Science, Jadavpur, Calcutta 700032, India

ARTICLE INFO

Article history:
Received 29 June 2011
Received in revised form 1 October 2011
Accepted 1 October 2011
Available online 8 October 2011

Keywords:
Electron ionization
Cross-section
Fragmentation
Mass-spectrometry
α-Cyclohexanedione

ABSTRACT

Electron ionization cross-section and fragmentation behavior of a volatile organic compound, 1,2-Cyclohexanedione (α-CHD) have been studied. Intact molecular ion is the major feature of the mass spectrum at low electron kinetic energy. However, with increasing energy of the ionizing electrons, molecular ion signal monotonically decreases and the fragment ions display some interesting variations. Three primary fragmentation channels, carbon monoxide and ketene losses and symmetric cleavage of the molecular ion have been identified. The ionization cross-sections of α-CHD have been estimated relative to that of molecular oxygen for electron kinetic energy in the range of 10–30 eV. Total ionization cross-section of the molecule has been estimated to be of the order of $\sim 10^{-16}$ cm^2/molecule. Electronic structure calculation at DFT/B3LYP/6-311++G** level has been performed for structural information of the intact molecular and fragment ions, and to calculate the thermodynamic parameters associated with various reaction channels. The predictions are found to useful to interpret the fragmentation spectra as a function of electron kinetic energy.

1. Introduction

Low molecular weight carbonyl compounds of bio- as well as anthropogenic origins belong to the category of volatile organic compounds (VOCs). These classes of compounds greatly influence the chemistry of earth's atmosphere [1–5]. In the lower region of troposphere, these compounds react with hydroxyl radical (OH), ozone and nitric oxide, and in upper atmosphere they undergo photo-degradation upon absorption of ultraviolet photons of solar radiation [6–17]. The latter process is extremely important as the organic radicals produced upon photolysis can initiate various reactions and produce more lethal substances in lower altitudes. Therefore studies of gas-phase dissociation of the carbonyl compounds by ultraviolet light or low-energy charge particles like electrons are extremely important. In this paper, we report for the first time the fragmentation behavior of a volatile dicarbonyl compound, α-CHD, upon ionization by low-energy electrons, and also report ionization cross-sections of the molecule measured at a range of low electron kinetic energies (e-KE).

The electron ionization and fragmentation behavior of small cyclic monoketones, e.g., cyclopentanone and cyclohexanone have been studied before [18]. However, the kinetic energy of ionizing electrons used in those studies was always 70 eV. In the dominant fragmentation channel for both ketones, a resonance stabilized ion of $m/z = 55$ is formed. This fragment ion is produced via α-cleavage of the molecular ions followed by a H-atom migration, and loss of $CH_3CH_2^\bullet$ and $CH_3CH_2CH_2^\bullet$ radicals for cyclopentanone and cyclohexanone, respectively. For the latter molecule, an intense ion peak appears for $m/z = 42$, and this happens as a result of successive loss of ethylene and carbon monoxide from the parent molecular ion. Cyclopentanone, has also been subjected to a number of photoionization/fragmentation studies. Baba et al. measured the photoionization mass spectra by exciting with 193 and 248 nm excimer lasers [19], and a series of fragment masses corresponding to loss of CO, HCO, C_2H_4, CH_3CO and CH_3CHO were identified. Kosmidis et al. have studied the process upon two-photon excitations to 3p and 3d Rydberg states in a molecular beam [20]. Recently Wang et al. carried out a very comprehensive study on femtosecond laser ionization/dissociation of cyclopentanone in a supersonic nozzle expansion [15]. Two wavelengths, 394 and 788 nm of the laser fields of pulse duration 90 fs and laser power in the range of 3×10^{13} to 4×10^{14} W/cm^2 were used. The dissociation pattern exhibited distinct excitation wavelength dependence. Ab initio electronic structure as well as RRKM calculations were carried out to interpret the observations.

Among the α-diketo compounds, the electron ionization fragmentation behavior of several linear analogues, e.g., 2,3-pentanedione, 3,4-hexanedione and 2,3-butanedione, have been studied recently [21]. Most of the measurements were carried out in MS/MS mode, where fragmentation of the mass selected molecular ions were carried out using collision induced dissociation scheme. In the case of 2,3-pentanedione, it was found that the loss of CO and C_2H_4 from the molecular ion occur in energetically competitive pathways resulting in formation of fragments, $CH_3COCH_2CH_3^+$

* Corresponding author.
E-mail address: pctc@iacs.res.in (T. Chakraborty).

1387-3806/$ – see front matter © 2011 Elsevier B.V. All rights reserved.
doi:10.1016/j.ijms.2011.10.001

and $CH_3C(OH)=C=O^+$, respectively. An important attribute that was revealed in those studies is that the α-diketo cations could be considered as one electron bound diacylium ion complex [22]. Secondly at low internal energy of these ions McLafferty rearrangement has also found to be a common process.

The molecule selected for present study, α-CHD, is an important structural subunit of an anticancer drug Quassinoid Bruceantin and anti-tumor steroid 4-hydroxyandrost-4-ene-3, 17-dione [23–25]. The α-methyl substituted CHD is a natural product responsible for the aroma of coffee beans. Being volatile, those compounds are easily released into the atmosphere, and thus important from the viewpoint of atmospheric chemistry. Under ambient conditions, the cyclic α-diketones also exists in enol tautomeric form, and the keto-enol equilibria of these molecules have been studied extensively [26]. Various experimental methods have been employed to elucidate the tautomeric forms of α-CHD assumed under different physical conditions. For example, electron energy loss spectroscopy shows that in the gas phase the molecule remains exclusively in the enolic form [27]. The same conclusion was also achieved on performing ion cyclotron resonance mass spectrometry [28] and electron diffraction studies [29]. Very recently Samanta et al. have measured the FTIR spectra of α-CHD in the gas phase, CCl_4 solution and cold inert gas matrixes [30]. In all such conditions, the molecules were found to exist exclusively in enol tautomeric form. On the other hand, in the neat solid crystal, experimental data suggest that a considerable fraction of the molecules could exist in diketo tautomeric form. Recently we have measured the ultraviolet (254 nm) photodissociation spectra of α-CHD in the gas phase [31].

The results of the present study are reported here in the following sequence. First, a brief description of the experimental and theoretical methods used is given. Since the molecular ion can exist in several possible isomeric forms, we have discussed the relative stabilities of those forms as a function of some key geometric

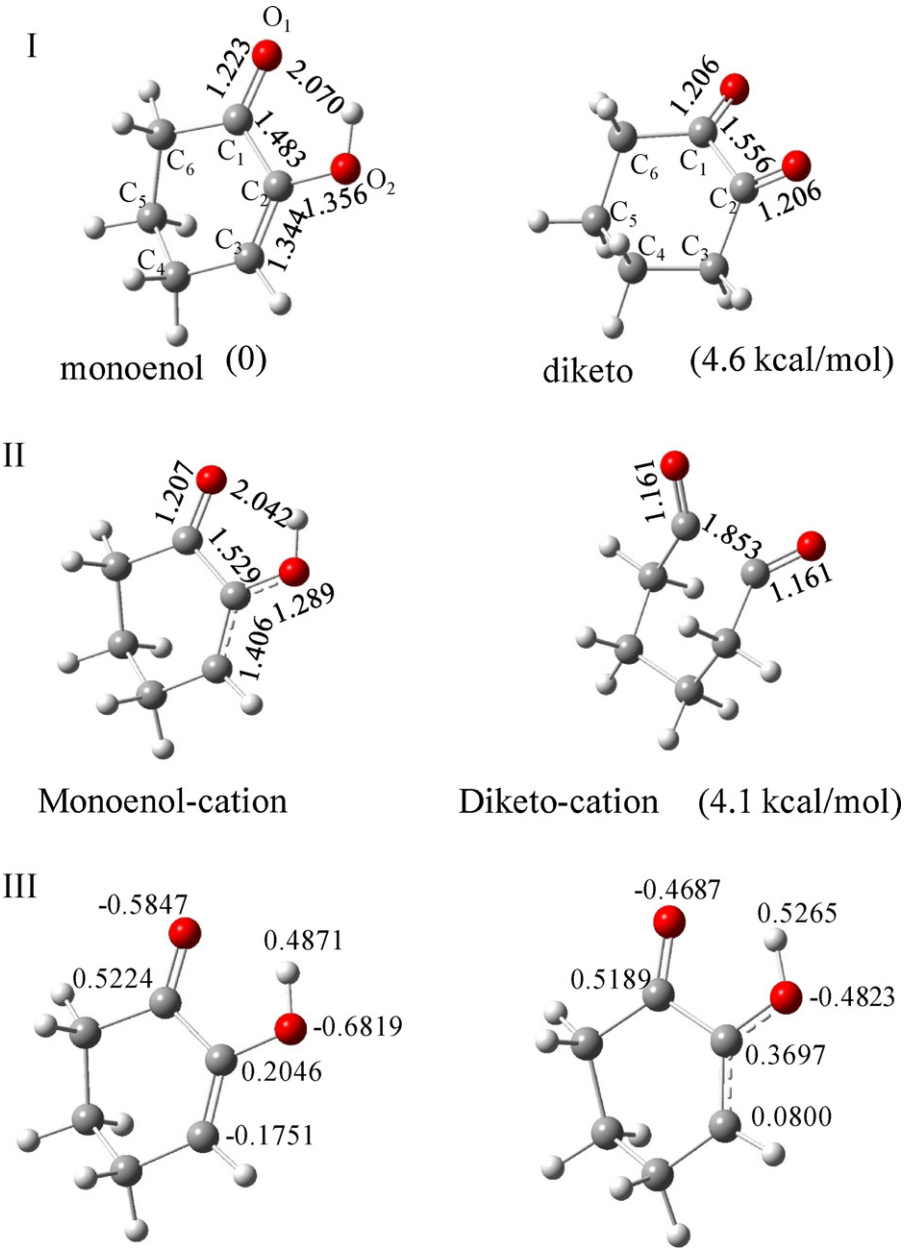

Fig. 1. Optimized geometries of the neutral (panel-I) and cationic forms (panel-II) of the enol and diketo tautomers of α-CHD calculated at DFT/B3LYP/6-311++G** level. Panel III shows natural charges on selected atoms of α-CHD obtained by performing NBO analysis on the optimized (DFT/B3LYP/6-311++G**) structures of neutral and molecular ion.

parameters predicted by electronic structure calculation. Then the experimental results are presented, different fragment ions are assigned and their possible formation channels have been discussed. Finally we have presented the data for the low-energy electron ionization cross-section of the molecule.

2. Experimental and theoretical method

2.1. Experimental

The experimental setup consists of a two stage vacuum chamber. The first chamber is equipped with an effusive/supersonic nozzle and is evacuated by a 6 in. oil diffusion pump. The second chamber houses the quadrupole mass spectrometer and it is evacuated by a 550l/s capacity turbo molecular pump (Pfeiffer vacuum). Both the pumps are backed by mechanical rotary pumps. Following the gas expansion, the molecular beam is introduced into the mass spectrometric chamber through a skimmer of orifice diameter 3 mm. The orifice diameter of the effusive nozzle (cw) is 100 μm and that of supersonic nozzle is 500 μm. The working pressure in the expansion chamber is typically $\sim 3.0 \times 10^{-6}$ mbar.

Our mass spectrometer is a flange mounted single quadrupole purchased from Extrel (Model MAX500). The mass analyzer consists of four cylindrical rods of diameter 19 mm and operated at a rf frequency of 1.2 MHz. An axial electron ionizer and a lens assembly to accumulate and focus the ion beam into the quadrupole are mounted at the top of the mass analyzer. The detector assembly is mounted in the post analyzer region, and it consists of a conversion dynode and a channeltron electron multiplier. The positive ions hit the dynode and the generated secondary electrons are detected by the electron multiplier. The dynode is biased by −5 kV. The software package Merlin Automation provided by Extrel was used to control the equipment and also for data acquisition and data processing.

The sample α-CHD was procured from Sigma–Aldrich (97%) and purified further by vacuum sublimation.

2.2. Theoretical

Geometry and stability of different isomeric forms of the parent molecular ion and fragments were calculated theoretically using density functional theory method using B3LYP functional and 6-311++G** basis set [32]. The neutrals and ionic species with closed shell electronic configurations were optimized using restricted B3LYP (RB3LYP) method and species with open shell electronic configuration were optimized using unrestricted B3LYP (UB3LYP) option. The frequencies for the vibrational normal modes were calculated at the same level to verify if an optimized geometry corresponded truly to a minimum on the potential energy surface. Gaussian G03 program package was used to perform all the calculations reported here [33].

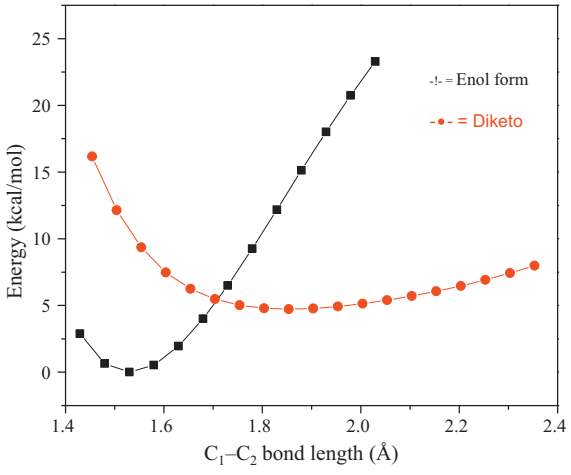

Fig. 2. Variation of relative energies of the diketo and enol tautomers of α-CHD cation with increase of C_1–C_2 bond length calculated at DFT/B3LYP/6-311++G** level. The curves represented by (-!-) and (–●–) symbols correspond to the cations of enol and diketo tautomers, respectively. For both cases, partial optimizations were performed by increasing the bond lengths in steps of size 0.05 Å.

3. Result and discussion

3.1. Isomeric structures of the parent molecular ion

In a recent infrared spetroscopic study, Samanta et al. have shown that in the gas phase α-CHD (neutral) exists exclusively

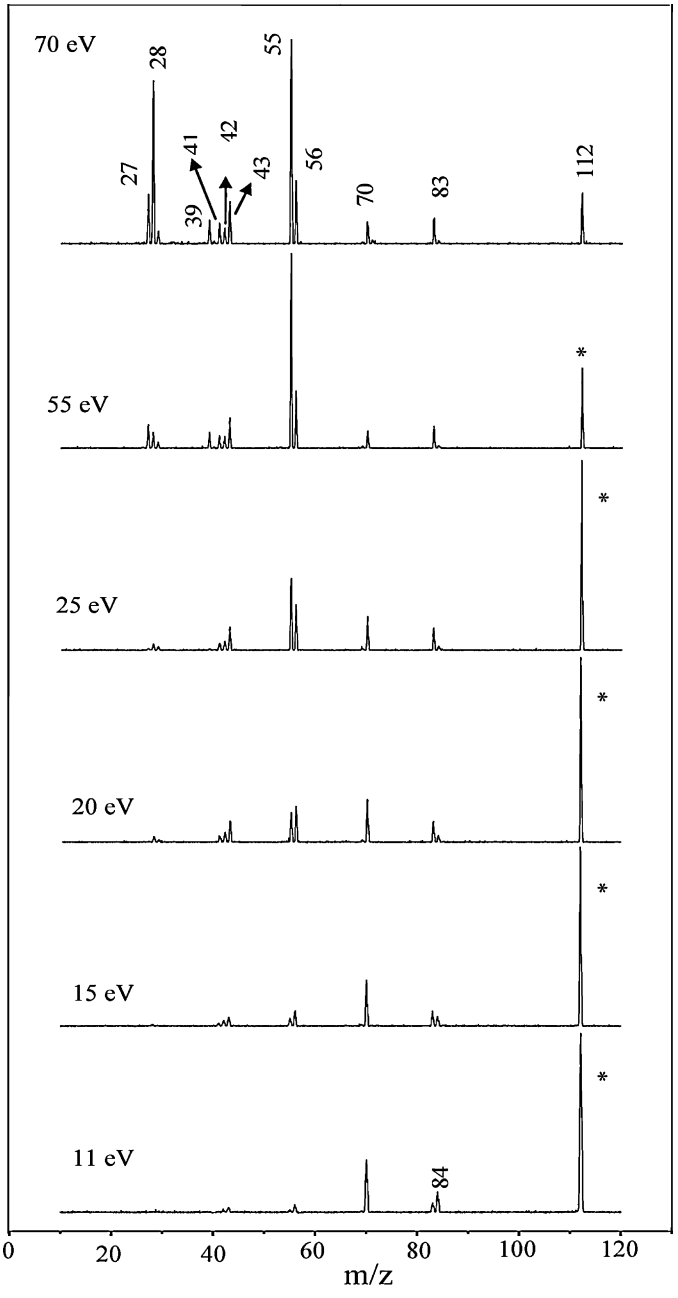

Fig. 3. Mass spectra of α-CHD for electron kinetic energies in the range of 10–70 eV.

in monoenol tautomeric form instead of diketo (Fig. 1, panel-I). The former gets stability over the latter owing to the presence of an intramolecular hydrogen bond. Geometry optimization of the molecular ion (cation) shows that enol tautomeric form is still more stable than diketo. However, geometric parameters (Fig. 1) are significantly altered by ionization. As predicted, C_1–C_2 bond length increases from 1.483 to 1.529 Å, C_2–O_2 bond length is shortened from 1.356 to 1.289 Å, and the bond order of C_2=C_3 (double bond) is reduced and the bond length is increased from 1.344 to 1.406 Å. However, the intramolecular $O_1\cdots H$ hydrogen bond length is shortened, which is primarily responsible for energy lowering of the enol form of the ion over the diketo tautomer. The experimental data presented below indicate that the cleavage of C_1–C_2 bond (α-cleavage) is the primary chemical event of the molecular ion, and the optimized structural parameters are also consistent with this chemical event. Interestingly, the tautomeric preference is sharply altered as C_1–C_2 bond breaks (Fig. 2). The calculation predicts that as the separation between C_1 and C_2 atoms increases, the energy of the enol tautomer increases sharply compared to diketo tautomer. Apparently, the origin of this behavior is due to weakening of the intramolecular hydrogen bond of the enol cation as the C_1–C_2 bond breaks apart. As the prediction indicates, the latter process should become more efficient as the internal energy of the produced ion becomes larger. Thus, one can infer that with increase in internal energy of the molecular ion, the tautomeric preference would be altered from enol to diketo. Furthermore, the predicted ionization energy of α-CHD is 8.6 eV and the minimum kinetic energy of electron that can be used in our experiment is 10 eV. Therefore, it is likely that the molecular ions will be generated with excess internal energy, and as argued, the preferred tautomeric form of the generated molecular ion will be diketo. Therefore, for analysis of our experimental data (presented below) only the diketo tautomeric form of the molecular ions has been considered. In the following section the probable structures of various fragment ions and their stabilities are discussed.

3.2. Mass spectra of α-CHD cation

The mass spectra recorded for different kinetic energies of the impinging electrons are presented in Fig. 3. Each spectrum is normalized with respect to the most intense mass peak in the spectrum. The lowest kinetic energy used in our measurement is 10 eV. Between 10 and 30 eV electron kinetic energies, the peak corresponding to the parent molecular ion appears as the base peak. Beyond 30 eV, the intensity of the molecular ion decreases with respect to other fragments, and the latter are also altered with electron kinetic energy. Analyzing various fragment masses we propose the following three major primary reaction channels.

Scheme: Primary dissociation channels of α-CHD proposed analyzing the mass spectra for different e-KE.

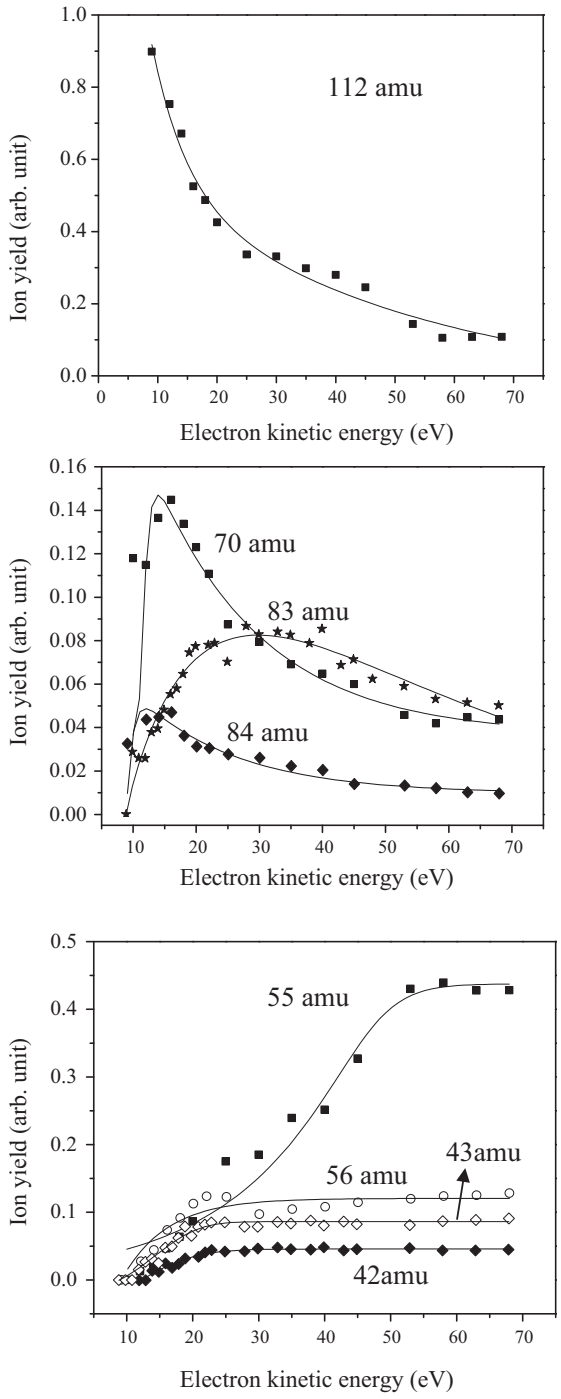

Fig. 4. Variation of ion yield of few selected ions for changing of e-KE. Top panel shows variation of molecular ion. Middle panel shows variation of fragment ions of masses 84, 83 and 70 amu. Bottom panel shows variation of fragment ions of masses 56, 55 and 43 amu.

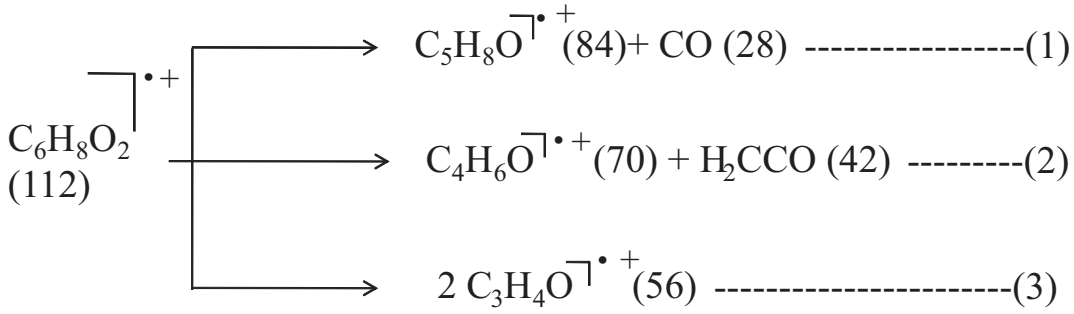

1. Molecular ion ($C_6H_8O_2^+$, m/z = 112 for z = 1): The ionic species corresponding to the mass of the parent molecular ion can exist in several isomeric forms depending upon the internal energy. It has been argued before that in the gas phase the neutral precursor exists exclusively in monoenol tautomeric form. For ionization to occur, the electrons are knocked out either from the keto or enolic oxygen. The natural charges on different atoms of the neutral and cation of α-CHD (enol) obtained from NBO analysis are shown in Fig. 1 (panel-III). It is seen that the positive charge of the cation is delocalized over the entire constituents of the molecule, and it is maximum on enolic O–H group. On ionization, the charge on H atom is increased by +0.04 and negative charge on oxygen is reduced by 0.19. At the Frank-Condon level, i.e., immediately on ionization the cation is produced in enol form, and theoretical calculation predicts that the enolic cation is energetically favoured over diketo. However, as explained before, this situation changes with increase in internal energy of the ion, and shown in Fig. 2 that after α-cleavage (C_1–C_2 bond) diketo tautomeric form of the ion is turned out to be more favoured as the two keto ends fall apart. Therefore, under the measurement condition, depending upon the internal energy distribution, the molecular ion could either be in open or closed form. Fig. 4 shows how the relative abundance of the molecular ion changes with kinetic energy of the impinging electrons. At higher electron kinetic energies, the molecular ions are produced with excess vibrational energy and undergo fragmentation at higher efficiency.

In Table 1 we have presented thermodynamic parameters corresponding to various ionic fragments which are produced from the molecular ion in primary reaction channels, i.e., when the e-KE are low. It is interesting to note that the intensity of various peaks in the mass spectrum correspond with thermodynamic stabilities of those fragments.

2. $C_5H_8O^{\bullet+}$ (84) and $C_5H_7O^+$ (83): Two weak peaks for m/z = 84 and 83 show up at the lowest electron kinetic energy (10 eV), but with increasing e-KE the peak intensity of 84 mass becomes weaker but the other (83) appears more prominent. We assign the former to a radical cation produced upon CO loss and the latter to that produced upon HCO loss from the parent molecular ion. The HCO loss could occur as due to successive loss of CO and H, or it can occur as loss of HCO radicals following a H atom migration from C_3 to C_1 atom of the open diketo cation, after α-cleavage. In Fig. 4 it is shown how the intensities of the two ion peaks change with e-KE.

Four different radical cations corresponding to mass 84 are considered and their structures optimized using DFT/B3LYP/6-311++G** theoretical method are presented in Fig. 5 (panel-I). Among these, cyclopentanone cation (A) is energetically most stable, and this is produced upon CO loss from the open chain diketo tautomeric form of the parent molecular ion and subsequent ring closure. Structure B corresponds to the cation of propyl ketene, and energetically it is favoured next to cyclopentanone cation, and its formation requires migration of a H atom from C_3 to C_6 atom. The cationic species labeled C is formed by H atom migration between adjacent C_3 and C_4 atoms after CO loss. Structure D is the 4-pentenal cation, and its energy is largest among the four species considered. Formation of this species from open chain structure of the parent molecular ion requires a γ-hydrogen abstraction, which is Mc-Lafferty rearrangement, and its formation should be favoured when the internal energy content of the ion is low. From the thermodynamic data presented in Table 1 it is evident that formation of cyclopentanone cation is the most favoured reaction channel. The ionization energy of propyl ketene ($84^{\bullet+}$ radical cation) is least among the four isomeric structures considered, although thermodynamically, its formation is somewhat less favoured. Furthermore,

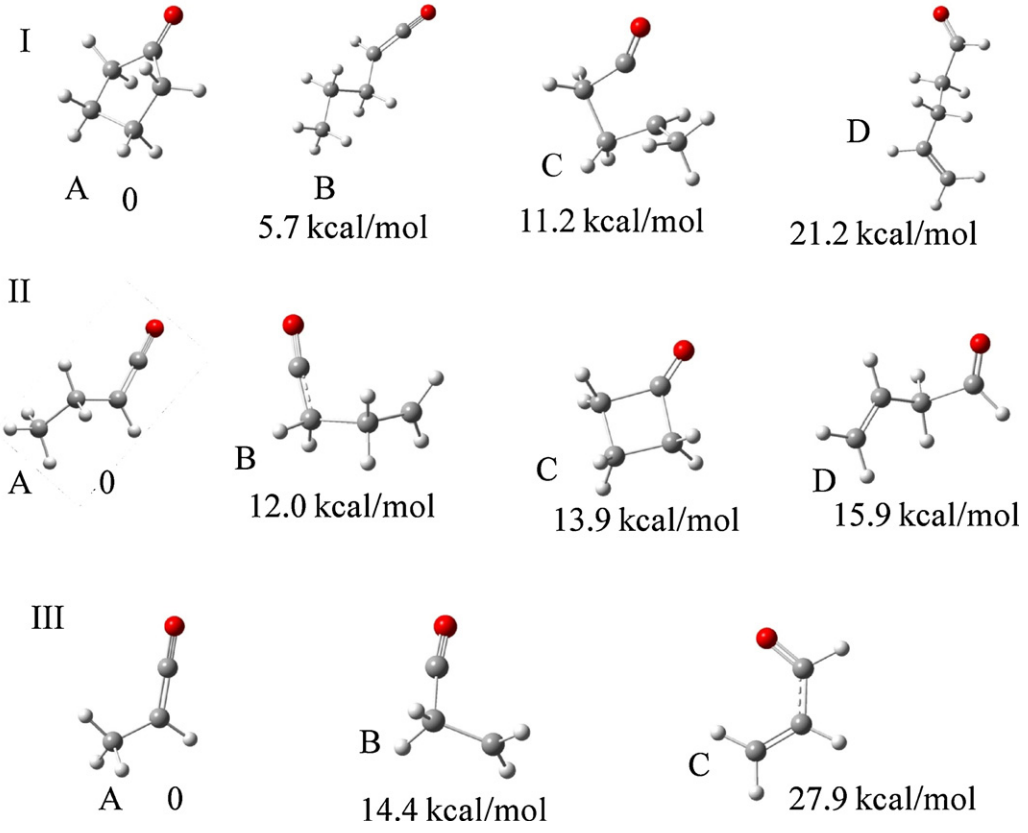

Fig. 5. Four probable structures of the fragment ions optimized at DFT/UB3LYP/6-311++G** level of theory. Top panel (panel-I) shows four different structures of mass 84 amu. Middle panel (panel-II) shows four different structures of mass 70 amu. Bottom panel (panel-III) shows three different structures of mass 56 amu.

Table 1
Calculated (DFT/B3LYP/6-311++G**) thermodynamic parameters (ΔH and ΔG) and ionization energies of the fragments produced in primary reaction channels.

Ion Diketo	Fragment ion	Neutral	$\Delta_r H^\circ$ (298 K) kcal/mol	$\Delta_r G^\circ$ (298 K) kcal/mol	IE (eV)
1,2CHD(112)	Cyclopentanone (84)	CO (28)	9.35	−1.39	9.3[d]
1,2CHD(112)	Propyl ketene (84)	CO (28)	15.2	1.88	8.49[a]
1,2CHD(112)	$CH_3CHCH_2CH_2CO$ (84)	CO (28)	19.98	7.26	8.78[a]
1,2CHD(112)	4-Pentenal (84)	CO (28)	30.13	16.75	9.14[e]
1,2CHD(112)	$CH_3CHCHCH_2CO$ (83)	HCO	101.04	88.09	
1,2CHD(112)	Ethyl ketene (70)	CH_2CO (42)	30.32	15.58	8.80[b]
1,2CHD(112)	$CH_2CH_2CH_2CO$ (70)	CH_2CO (42)	41.48	26.54	
1,2CHD(112)	Cyclobutanone (70)	CH_2CO (42)	43.61	29.74	9.4 ± 0.1[c]
1,2CHD(112)	CH_2CHCH_2CHO (70)	CH_2CO (42)	45.56	30.54	9.27[e]
1,2CHD(112)	Methyl ketene (56)	CH_3CHCO (56)	34.73	20.47	8.95[b]
1,2CHD(112)	CH_2CH_2CO (56)	CH_3CHCO (56)	48.64	34.41	
1,2CHD(112)	CH_2CHCHO (56)	CH_3CHCO (56)	61.92	48.17	9.97[e]
1,2CHD(112)	CH_2CO (42)	CH_3CH_2CHCO (70)	55.11	40.49	9.62[a]

[a] Ref. [3].
[b] Ref. [34].
[c] Ref. [35].
[d] Ref. [36].
[e] Calculated at DFT/B3LYP/6-311++G**.

Table 2
Important thermodynamic parameters corresponding to secondary dissociation of the radical cation $84^{\bullet+}$.

Radical cation (m/z = 84)	Radical cation/cation	Radical/neutral	$\Delta_r H^\circ$ (298 K) kcal/mol	$\Delta_r G^\circ$ (298 K) kcal/mol
Cyclopentanone$^{\bullet+}$	H_2CCHCO^+ (55)	$H_3CCH_2^\bullet$ (29)	39.4	24.5
	$H_3CHCCO^{\bullet+}$ (56)	H_2CCH_2 (28)	29.7	15.7
Propylketene$^{\bullet+}$	$H_2CCHCHO^{\bullet+}$ (56)	H_2CCH_2 (28)	56.9	43.4
4-Pentenal$^{\bullet+}$	$H_2CCO^{\bullet+}$ (42)	H_3CHCH_2 (42)		
	H_2CCHCO^+ (55)	$H_3CCH_2^\bullet$ (29)	33.6	21.2
	HCO^+ (29)	$H_2CCHCH_2CH_2^\bullet$ (55)	61.8	50.9
	H_3CCO^+ (43)	$H_2CCHCH_2^\bullet$ (41)	6.3	−4.8
Structure (C)$^{\bullet+}$	$H_2CCO^{\bullet+}$ (42)	H_3CHCH_2 (42)	33.1	21.1

also from thermodynamic viewpoint, formation of 83^+ cation ($CH_3CH=CHCH_2CO^+$) seems to be highly unfavourable.

A notable behavior of the $84^{\bullet+}$ radical cationic species is that it is extremely fragile and its peak intensity decays very quickly with increase in e-KE (Fig. 4). On the other hand, the intensity of the mass peak at 83 gradually increases with e-KE and well survives up to 70 eV. The probable secondary fragmentation channels of the four isomeric species (Fig. 5, panel-I) are listed in Table 2 along with the calculated thermodynamic parameters. According to these energetic parameters, the fragment ion of mass 43 (Fig. 4) could most easily be produced via dissociation of 4-pentanal radical cation to $H_3C–CO^+$ (43) and $H_2CCHCH_2^\bullet$ (41). On the other hand, the cationic species of mass 55 (CH_2CHO^+) is favoured most at higher e-KE, and it is more easily formed by dissociation of propyl ketene radical cation. Cyclopentanone cation being very stable its dissociation to CH_2CHO^+ (55) is relatively less favoured, but possible at high e-KE.

3. $C_4H_6O^{\bullet+}$ (m/z = 70): At low e-KE the intensity of this fragment ion peak is just next to that of the molecular ion peak and as shown in Fig. 4 the intensity is maximum for e-KE ∼ 15 eV and drops sharply with increase in electron energy. We assign it to a radical cation produced as a result of ketene loss from the open diketo radical cation of α-CHD. Four isomeric structures for the species of molecular formula $C_4H_6O^+$, m/z = 70, for z = 1 are suggested and their optimized geometries and relative energies, predicted by electronic structure calculation, are shown in Fig. 5 (panel-II).

Among the four isomeric cations, ethyl ketene (A) is energetically most stable. The isomers B and C are basically the closed and open chain forms of the same cation, and both can easily be dissociated into a ketene and ethylene. The formation of the species D requires a H atom shifting from C_1 to C_3 of the open chain α-CHD diketo cation before ketene loss. Energetically this species is least favoured, and a H-atom loss from this species could be a very feasible reaction channel. However, absence of 69 mass peak in the mass spectrum indicates that species D is not produced. The thermodynamic data presented in Table 1 indicates that ethyl ketene production is favoured among the four $70^{\bullet+}$ radical cation production channels.

The secondary fragment ions that could be generated from $70^{\bullet+}$ are listed in Table 3. Ketene (42), carbon monoxide (28), HCO^+ (29) and acetyl radical (43) could be produced from different isomeric structures. Production of carbon monoxide cation is highly endothermic process. Dissociation of structure $C^{\bullet+}$ via this channel should be energetically unfavourable.

Table 3
Important thermodynamic parameters corresponding to secondary dissociation of the radical cation $70^{\bullet+}$.

Radical cations (m/z = 70)	Radical cation/cation	Radical/neutral	$\Delta_r H^\circ$ (298 K) kcal/mol	$\Delta_r G^\circ$ (298 K) kcal/mol
A$^{\bullet+}$	$H_2CCO^{\bullet+}$ (42)	H_2CCH_2 (28)	38.3	28.1
Cyclobutanone$^{\bullet+}$	$H_2CCO^{\bullet+}$ (42)	H_2CCH_2 (28)	25.6	13.9
C$^{\bullet+}$	$H_2CCO^{\bullet+}$ (42)	H_2CCH_2 (28)	27.7	17.2
	$C{\equiv}O^{\bullet+}$ (28)	$H_2C{=}CH–CH_3$ (42)	116.2	106.5
		$CH_2{=}CH–CH_2^\bullet$ (41)		
D$^{\bullet+}$	HCO^+ (29)		43.5	34.1
	CH_3CO^+ (43)	$CH{=}CH_2^\bullet$ (27)	34.3	23.5

4. $C_3H_4O^{\bullet+}$ ($m/z = 56$) and $C_3H_3O^+$ ($m/z = 55$): Via symmetric rupture, the open chain diketo form of α-CHD can produce two identical fragments of mass (56) and the positive charge will be retained on either of the fragments. Fig. 4 indicates that the relative abundance of the species does not increase with e-KE beyond 20 eV, and its relative yield is also not very high. The cation that is most abundantly formed at higher values of e-KE is of mass 55, and we have assigned it to a species of structure $(^{\bullet}O{\equiv}C{-}CH{=}CH_2)^+$. This species could be produced from the diketo form of molecular ion in several possible channels. A symmetric rupture followed by an H atom loss would produce cation of mass 55. The species of mass 56 could also be produced from the parent molecular ion via successive loss of CO and $CH_2{=}CH_2$. Three possible isomeric structures corresponding to mass 56 are shown in Fig. 5 (panel-III).

   Structure A corresponds to methyl ketene cation produced on hydrogen atom shift in the cationic moiety of the symmetric fragment. Structure B (Fig. 5, panel-III) is the species produced by direct dissociation of the molecular cation about the C_4–C_5 bond. It cannot be very stable, and could dissociate into CO and C_2H_4. However, the Fig. 4 shows the species is quite stable and we rule out the possibility for the structure B. Furthermore, it has been shown previously that the cation of mass 56 can be generated from cyclopentanone cation via secondary dissociation through energetically favourable reaction channel. Structure C is acrolein cation, which is ~28 kcal/mol higher in energy compared to the former.
5. $C_2H_3O^+$ ($m/z = 43$) and $C_2H_2O^{\bullet+}$ ($m/z = 42$) cation: We have assigned the cationic species of mass 43 to $CH_3{-}C{\equiv}O^+$, and it could be generated in secondary fragmentation channels from 4-pentenal$^{\bullet+}$ ($m/z = 84$) and also from the radical cation of mass $70^{\bullet+}$ (structure D). From energetic viewpoint, the latter channel for its formation seems quite feasible (Table 3). The ion yield of 43^+ cation increases (Fig. 4) with increasing e-KE. We assign the cationic species corresponding to mass 42 as of ketene cation. In Fig. 4 it is shown that with the increase in e-KE, the ion yield of the species is increased slowly but its relative abundance is quite small. The obvious reasons are, first the ionization energy of ketene is larger compared to other fragments. The reaction is highly exothermic as a result probability of its survival as intact ion is small. With increasing electron kinetic energy the intensities of lower mass fragments appear enhanced. This behavior is quite general and consistent with the concept that at low kinetic energy the positive charge will reside preferentially on higher mass fragments, but at higher values of e-KE the charges could reside on the lower mass fragments as well.

3.3. Cross section determination

In the present study, the ionization cross section of α-CHD has been determined with respect to molecular oxygen. In many previous studies atomic gases like Xe (IE ~ 13 eV) and argon (IE ~ 15.76 eV) were used. Here, oxygen has been preferred as a reference, because, first it is a molecule, and secondly, its ionization energy is closer to that of α-CHD (IE ~ 12.06 eV). In our experimental arrangement the vapour of α-CHD and molecular oxygen were mixed at ratios of 1:0.3 and 1:0.5, and the gas mixture were introduced into the expansion chamber through a continuous beam nozzle orifice (dia ~ 100 μm). The relative ionization cross sections are measured by varying e-KE in the range of 10–28 eV.

The following working relation has been used to estimate the relative ionization cross-section of the molecule (σ(M))

$$\sigma(M) = \sigma(O_2)\frac{P(O_2)}{P(M)}\frac{I(M)}{I(O_2)}\frac{M}{32}.$$

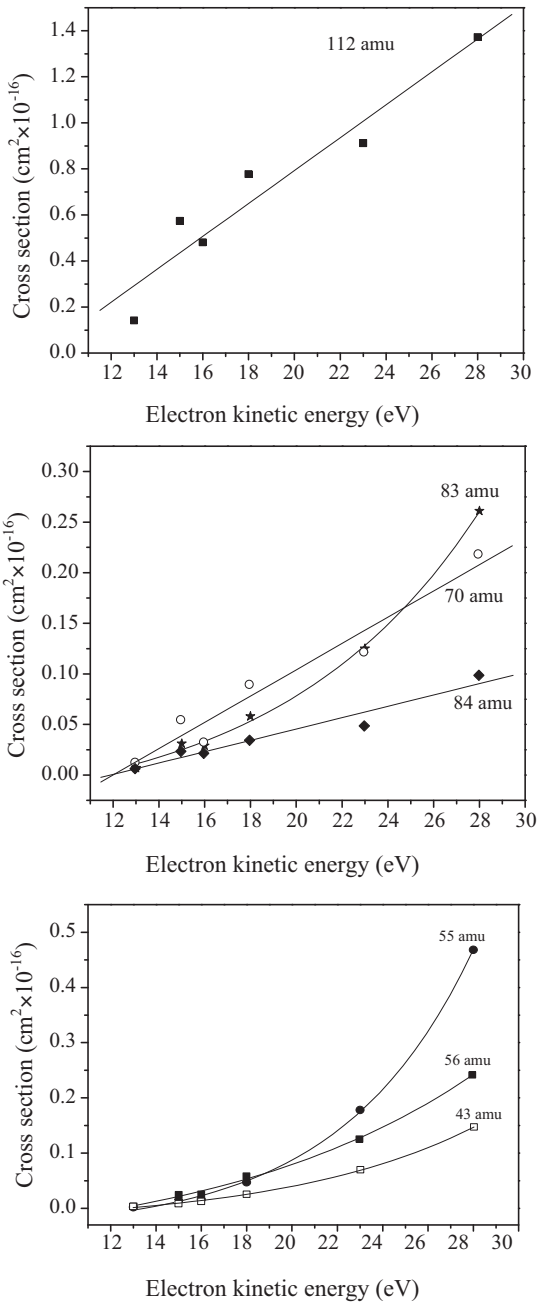

Fig. 6. Variation of ionization cross-sections of molecular and selected fragment ions as a function of e-KE.

Here $\sigma(O_2)$ is the ionization cross section of molecular oxygen, $P(O_2)$ and P(M) are partial pressures of oxygen and sample in the mixing chamber, respectively. I(M) and $I(O_2)$ are the intensities of mass peaks corresponding to a species of mass M and molecular oxygen, respectively. In Fig. 6 the relative ionization cross-sections estimated for all the fragment ions are presented. The total ionization cross-section for each value of e-KE has been estimated by summing the cross section for each fragment ions. At 28 eV the molecular ion contributes 43% (Fig. 7) of the total ionization cross section and this contribution decreases with increasing kinetic energy of electron from 13 to 28 eV. The behavior can be compared with those reported for e-KE dependence of ionization cross-sections for acetone, 2-butanone and 2-heptanone, and for these cases the cross-sections reach to a saturation level for e-KE in

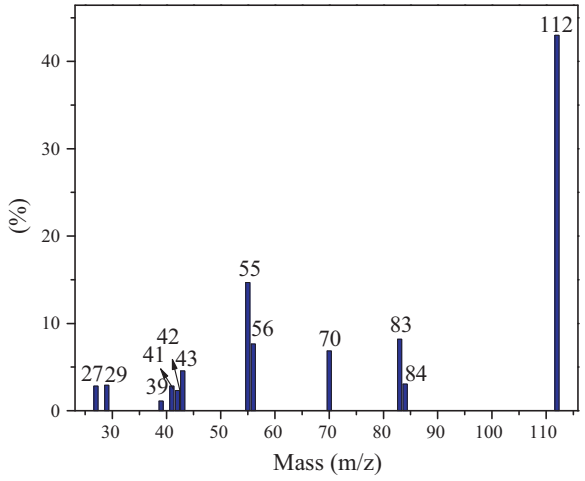

Fig. 7. Contributions (%) of various fragment ions to the total ionization cross-section at 28 eV.

the range of 35–40 eV. The contributions of various fragment ions of α-CHD in the total ionization cross-sections are shown in Fig. 7.

3.4. Summary

In this paper we have presented for the first time the electron ionization mass spectra of α-CHD by varying the electron kinetic energy in the range of 10–30 eV. At low e-KE, fragment ions produced due to loss of carbon monoxide and ketene are the most favoured dissociation channels. However, on increasing e-KE, these ions undergo secondary fragmentation. Electronic structure calculation predicts that an enol tautomeric form is energetically preferred both for the neutral and cationic states of α-CHD. However, after α-cleavage (rupture of C_1–C_2 bond), the diketo tautomer turns out to be the lower energy tautomeric species. The ionization cross-section of α-CHD has been estimated with respect to molecular oxygen (O_2) for e-KE values up to 30 eV.

Acknowledgements

The authors sincerely thank the Department of Science and Technology, Government of India for financial support to carry out the research presented here. AM thanks CSIR for Senior Research Fellowship and AKG thanks CSIR for Junior Research Fellowship.

References

[1] R. Koppmann, Volatile Organic Compounds in the Atmosphere, Blackwell Publishing Ltd., 2007.
[2] D.J. Jacob, Introduction to Atmospheric Chemistry, Princeton, New Jersey, 1999.
[3] J.R. Vacher, F. Jorand, N. Blin-Simiand, S. Pasquiers, Int. J. Mass Spectrom. 273 (2008) 117.
[4] J.R. Vacher, F. Jorand, N. Blin-Simiand, S. Pasquiers, Int. J. Mass Spectrom. 240 (2005) 161.
[5] S. Szopa, B. Aumont, S. Madronich, Atmos. Chem. Phys. 5 (2005) 2519.
[6] R. Atkinson, Atmos. Environ. 34 (2000) 2063.
[7] R. Atkinson, J. Arey, Chem. Rev. 103 (2003) 4605, and references therein.
[8] R. Atkinson, E.C. Tuazon, S.M. Aschmann, Environ. Sci. Technol. 34 (2000) 623.
[9] R. Atkinson, S.M. Aschmann, J. Phys. Chem. 92 (1988) 4008.
[10] T.J. Wallington, M.J. Kurylo, J. Phys. Chem. 91 (1987) 5050.
[11] C. Zhu, L. Zhu, J. Phys. Chem. A 114 (2010) 8384.
[12] G.K. Moortgat, H. Meyrahn, P. Warneck, Chem. Phys. Chem. 11 (2010) 3896.
[13] M. Araujo, B. Lasorne, M.J. Bearpark, M.A. Robb, J. Phys. Chem. A 112 (2008) 7489, and references therein.
[14] B. Rajakumar, T. Gierczak, J.E. Flad, A.R. Ravishankara, J.B. Burkholder, J. Photochem. Photobiol. A: Chem. 199 (2008) 336.
[15] Q. Wang, D. Wu, M. Jin, F. Liu, F. Hu, X. Cheng, H. Liu, Z. Hu, D. Ding, H. Mineo, Y.A. Dyakov, A.M. Mebel, S.D. Chao, S.H. Lin, J. Chem. Phys. 129 (2008) 204302.
[16] Y. Haas, Photochem. Photobiol. Sci. 3 (2004) 6, and references therein.
[17] E.W. Diau, G.C. Kötting, T.I. Sølling, A.H. Zewail, Chem. Phys. Chem. 3 (2002) 57, and references therein.
[18] R.M. Silvertein, F.X. Webster, Spectrometric Identification of Organic Compounds, John Wiley & Sons. Inc., 2005.
[19] M. Baba, H. Shinohara, N. Nishi, Chem. Phys. 83 (1984) 221.
[20] C. Kosmidis, J.G. Philis, P. Tzallas, Phys. Chem. Chem. Phys. 1 (1999) 2945.
[21] X. Wang, J.L. Holmes, Int. J. Mass Spectrom. 249–250 (2006) 222.
[22] E.C. Meurer, F.C. Gozzo, R. Augusti, M.N. Eberlin, Eur. J. Mass Spectrom. 9 (2003) 295.
[23] S.M. Kupchan, R.W. Britton, J.A. Lacadie, M.F. Ziegler, C.W. Sigel, J. Org. Chem. 40 (1975) 648.
[24] N. Fukamiya, K. Lee, I. Muhammad, C. Murakami, M. Okano, Harvey, I.J. Pelletier, Cancer Lett. 220 (2005) 37.
[25] (a) K. Hoffken, W. Jonat, K. Possinger, M. Kolbel, T.H. Kunz, H. Wagner, R. Becher, R. Callies, P. Friederich, W. Willmanns, H. Maass, C.G. Schmidt, J. Clin. Oncol. 8 (1990) 875;
(b) T. Pickles, L. Perry, P. Murray, P. Plowman, Br. J. Cancer 62 (1990) 309.
[26] J.T. Francis, A.P. Hitchcock, J. Phys. Chem. 98 (1994) 3650.
[27] G. Bouchoux, Y. Hoppilliard, R. Houriet, New J. Chem. 11 (1987) 225.
[28] M.A. Gianturco, A.S. Giammarino, R.G. Pitcher, Tetrahedron 19 (1963) 2051.
[29] Q. Shen, M. Traetteberg, S. Samdal, J. Mol. Struct. 923 (2009) 94.
[30] A.K. Samanta, P. Pandey, B. Bandyopadhyay, T. Chakraborty, J. Mol. Struct. 963 (2010) 234.
[31] A. Mukhopadhyay, M. Mukherjee, A.K. Ghosh, J. Phys. Chem. A 115 (2011) 7494.
[32] A.D. Becke, J. Chem. Phys. 98 (1993) 5648.
[33] M.J. Frisch, G.W. Trucks, H.B. Schlegel, G.E. Scuseria, M.A. Robb, J.R. Cheeseman, V.G. Zakrzewski, J.A. Montgomery Jr., R.E. Stratmann, J.C. Burant, S. Dapprich, J.M. Millam, A.D. Daniels, K.N. Kudin, M.C. Strain, O. Farkas, J. Tomasi, V. Barone, M. Cossi, R. Cammi, B. Mennucci, C. Pomelli, C. Adamo, S. Clifford, J. Ochterski, G.A. Petersson, P.Y. Ayala, Q. Cui, K. Morokuma, D.K. Malick, A.D. Rabuck, K. Raghavachari, J.B. Foresman, J. Cioslowski, J.V. Ortiz, A.G. Baboul, B.B. Stefanov, G. Liu, A. Liashenko, P. Piskorz, I. Komaromi, R. Gomperts, R.L. Martin, D.J. Fox, T. Keith, M.A. Al-Laham, C.Y. Peng, A. Nanayakkara, M. Challacombe, P.M.W. Gill, B. Johnson, W. Chen, M.W. Wong, J.L. Andres, C. Gonzalez, M. Head-Gordon, E.S. Replogle, J.A. Pople, Gaussian 03, Revision E.01, Gaussian, Inc., Pittsburgh, PA, 2003.
[34] H. Bock, T. Hirabayashi, S. Mohmand, Chem. Ber. 114 (1981) 2595.
[35] G. Bieri, L. Asbrink, W. Von Niessen, J. Electron. Spectrosc. Relat. Phenom. 27 (1982) 129.
[36] E.F. Rothgery, J. Holt, H.A. McGee Jr., J. Am. Chem. Soc. 97 (1975) 4971.